Journal of Physics: Conference Series

PAPER • OPEN ACCESS

A study of cavitation erosion resistance of an ion nitrided titanium alloy by means of the vibration and rotating disk methods

To cite this article: V Safonov *et al* 2024 *J. Phys.: Conf. Ser.* **2710** 012023

A study of cavitation erosion resistance of an ion nitrided titanium alloy by means of the vibration and rotating disk methods

V Safonov[1,2], A Zykova[1], J Steller[2], M Szkodo[3], G Gajowiec[3] J Chmiel[4], A Varhoshkov[5] and I Klimenko[1]

[1] National Science Center "Kharkiv Institute of Physics and Technology",
1 Akademicheskaya St., 61108 Kharkiv, Ukraine
[2] Szewalski Institute of Fluid-Flow Machinery of the Polish Academy of Sciences,
14 J. Fiszera St., 80-231 Gdansk, Poland
[3] Gdańsk University of Technology, 11/12 Narutowicza St., 80-233 Gdańsk, Poland
[4] Maritime University of Szczecin, 1-2 Wały Chrobrego Av. 70-500 Szczecin, Poland
[5] Ionitech Ltd, 5 Kapitana Lyubena Kondakova St., Sofia 1582, Bulgaria

E-mail: safonov600@gmail.com

Abstract. In this work, a comparative analysis of the cavitation erosion resistance of the Ti–6.7Al–2.5Mo–1.8Cr–0.5Fe–0.25Si alloy (known as brand VT3-1) before and after low-temperature ion nitriding is carried out. Two test methods were applied, using vibrative (ASTM G-32) and rotating disk rigs, respectively. The kinetic dependences of the erosive destruction of samples of titanium alloy VT3-1 in the initial state, after ion nitriding and stainless steel AISI 321 were obtained. A study of the microstructure, hardness and surface morphology was carried out. The samples were examined using optical and scanning electron microscopy. The relationship between mass loss and cavitation erosion duration was experimentally determined and analyzed. The erosion rate on a rotating disk stand is much higher than during vibration tests. A large cavitation load gradient provides additional opportunities for analyzing the durability of materials and coatings using this method.

1. Introduction

The titanium alloys have various applications in the aerospace, chemical, marine, power supply, and automotive industries due to their high strength, as well as corrosion and heat resistance [1].

The ever-rising requirements on the performance of hydraulic machinery and equipment on the one hand and lowering the costs of new hydraulic installations or systems on the other one stand often in contradiction with the need to preserve their high resilience against cavitation threat, including cavitation erosion. Cavitation erosion is a common form of surface damage of the fluid-flow machinery such as turbines, impeller pumps, ship propellers, rudders, valves and other hydraulic equipment. Cavitation erosion is a challenging problem because of the associated huge economic losses and potential safety hazards [2].

Steam turbines are involved in the generation of more than 80% of worldwide electricity. One of the most promising directions for increasing their efficiency is the use of long titanium blades. Thus, the problem of droplet erosion of the blades becomes even more important due to the increase in their peripheral velocity.

The physical processes occurring during cavitation and drop impact are different. However, the general mechanism of erosion is that it occurs due to fatigue caused by repeated impulse loading, due to the impact of droplets or the collapse of cavitation bubbles. Erosion from both cavitation and liquid droplets goes through the same stages of incubation, acceleration, maximum velocity and steady state. Cavitation erosion data can also be used to predict droplet impact erosion because the correlation between both forms of erosion is very high [3, 4]. In general, understanding of the mechanisms and factors that increase the cavitation resistance of materials may be useful in preventing some other types of erosion. The counter-erosive properties of titanium alloys can be improved by various methods of surface hardening [5, 6, 7]. These include the application of functional coatings or surface modification by nitriding [8, 9].

The purpose of this study was a comparative analysis of the resistance to cavitation erosion of the VT3-1 alloy (GOST 19807-91 USSR Standard), as well as samples subjected to low-temperature ion nitriding in Ar and N_2 gas atmosphere using vibrative (ASTM Standard G-32) and rotating disk erosion test methods.

2. Materials and Methods

The study was carried out on samples of VT3-1industrial titanium (α+β) alloy. The alloy is used for machinery components operating for a long time at temperatures up to 450°C. The alloy shows a tensile strength σ_B > 1000 MPa, high corrosion resistance in the annealed and thermally strengthened states in a humid atmosphere, as well as sea water and many other aggressive environments.

Experimental studies of cavitation resistance were carried out on samples of titanium alloy before and after ion nitriding. Samples of titanium alloy and stainless steel were mechanically polished to 2000 grit with SiC sandpaper and sonicated in acetone. The reference material was stainless steel (SS) AISI 321. This material was extensively used within the International Cavitation Erosion Test Project [10]. It has also been used in our further rotating disk tests to check the erosive load stability.

Resistance to cavitation erosion was assessed by tests carried out at a rotating disk facility [11] in the laboratory of the IMP PAN (Szewalski Institute of Fluid-Flow Machinery) on samples with 30 mm diameter. Erosion-cavitation tests were also carried out at a vibrative rig located at the Maritime University of Szczecin. The test was performed in accordance with ASTM G-32 in a variant with a stationary sample in an environment of deionized water with a conductivity of less than 0.01 mS/cm. The rig is built on the basis of Sonics VCX-500 ultrasonic processor. The vibration amplitude and frequency of the horn tip were 50 micrometers (peak-to-peak) and 20 kHz, respectively, which corresponded to power of 36 to 40 W. The nominal stand-off distance between the horn tip and the sample surface was 0.5 mm. The temperature of water in the working vessel of 2 dm^3 volume was set at 25°C. The temperature was stabilized using a cooling system powered by a Polyscience ultra-thermostat with an accuracy of +/- 1 °C.

The nitriding process was carried out on an IONITECH industrial plasma installation ION-25I-SN-05. After evacuation, the chamber was purged with inert gas to remove residual air. The next stage was ion cleaning in a glow discharge for 15 minutes in pulsed mode with a duty cycle of electrical pulses of 50%. During the cleaning process, the discharge current was constant and amounted to 10-20% of the maximum value at voltage of 350 V, argon pressure of 50 Pa, temperature T = 150°C. Low current and low duty cycle prevent arc development. The purpose of this stage of processing is the final cleaning of the samples from any contaminants and the beginning of their heating to the nitriding temperature. The duty cycle of electrical pulses gradually increased to 80-90%. The pressure of the working mixture also increased, rising along with the temperature. After reaching the appropriate temperature, the stage of nitriding in the gas mixture began. The processing parameters were as follows: nitriding time 420 min; nitriding atmosphere (25% Ar–75% N2); total pressure 130 Pa and temperature 600°C.

The phase composition and microstructural characterization of the samples were studied by X-ray phase analysis using a PANalytical X'Pert Pro device with a copper anode. The microstructure was analyzed by optical and JSM-7800F (JEOL, Tokyo, Japan) scanning electron microscope (SEM). Mechanical properties such as hardness (H) and elastic modulus (E) of the the surface of the samples were determined by measuring indentation at low loads using a Nanoindenter G200 (USA). Indentation was carried out with a Berkovich diamond triangular pyramid. Analysis of load displacement curves was carried out using the Oliver and Farr method, which allows one to determine the values of physical and mechanical characteristics at the depth of penetration of the indenter.

3. Results and Discussion

X-ray diffraction analysis showed that after nitriding there was a predominant increase in the intensity of peaks from the α-Ti matrix phase. Reliable confirmation of the formation of the TiN phase in the modified layer has not been obtained.

At the same time, ion-plasma nitriding of the alloy led to an increase in the microhardness of the initial state from 3.6 GPa to 4.7 GPa. The mechanical characteristics of the samples measured by a nanoindenter before and after nitriding were as follows: H = 4.5 GPa, E = 155 GPa and H = 8 GPa, E = 140 GPa, respectively. The hardness distribution over depth was estimated based on a model for interpreting micro- and macro indentation data of thin coatings [12]. The thickness of the modified layer was 5 μm, the layer with a hardness of 8 GPa was about 1 μm.

As a result of six-hour tests at a rotating disk installation, cumulative weight loss curves for titanium samples, as well as reference samples SS, were obtained (figure 1). The erosion rate of samples depending on the test duration is shown in figure 2.

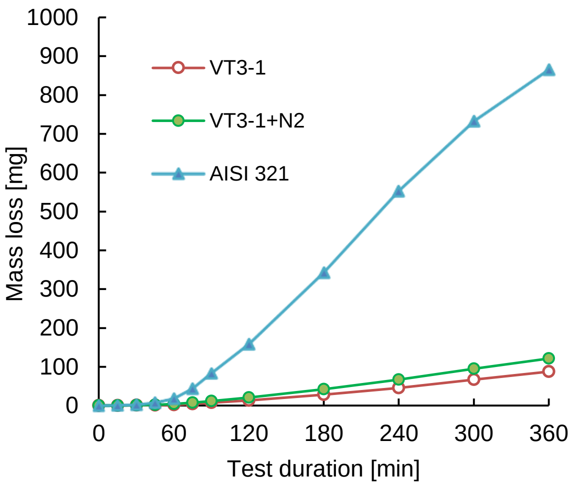

Figure 1. Cumulative mass loss of samples depending on testing time at the rotating disk.

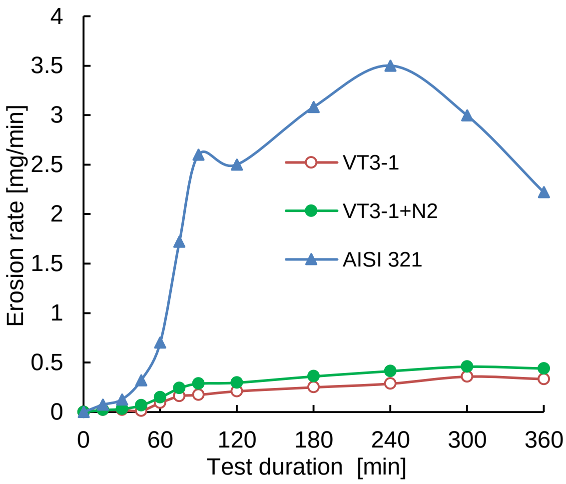

Figure 2. Erosion rate of samples depending on test duration at the rotating disk.

The dependences of the values of mass loss and erosion rate are close for the original titanium and for nitrided titanium. Similar dependencies were obtained for cavitation erosion using the vibration apparatus (figure 3, 4) but the values for both mass loss and erosion rate are significantly below. As can be seen from these data, an almost two-fold increase in the hardness of a titanium alloy after nitriding does not lead to an increase in cavitation resistance. The dependence of the erosion rate provides additional information about the intensity of the cavitation process. A decrease in the erosion rate after a certain maximum value indicates the stage of stabilization of the erosional relief and the transition to the stationary phase of the erosion process. The time to reach the maximum erosion rate is inversely proportional to the intensity of the cavitation load (figure 2 and figure 4).

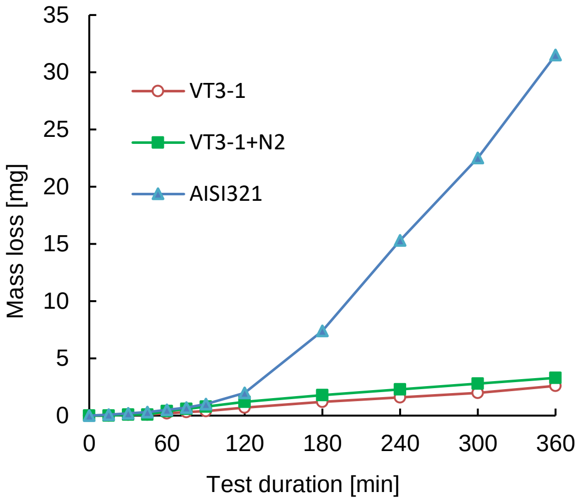

Figure 3. Cumulative weight loss of samples depending on test duration at the vibrative apparatus.

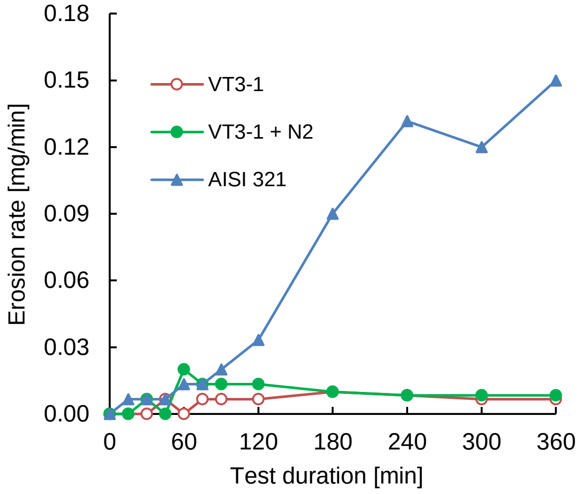

Figure 4. Erosion rate of samples depending on test duration at the vibrative apparatus.

Figure 5 shows the morphology of samples from the original titanium alloy, nitrided and SS steel after erosion tests at the rotating disk with different test times. The greatest damage is observed on stainless steel. As for the titanium alloy (figure 5, top), compared with the nitrided sample (figure 5, middle), the surface morphology of the original sample shows damage over a larger area in all times of trial.

Figure 5. Photographs of the rotating disk samples. Top - original titanium alloy, middle - ion nitriding titanium alloy and bottom - stainless steel after 15 min (a), 60 min (b) and 360 min test duration (c).

This indicates that the strengthened surface layer delays the development of erosion damage to the surface. Unlike the ductile original alloy, this layer is brittle, and cracks appear in it over time. After the destruction of the thin hardened layer, the erosion rates of the original and nitrided samples become the same.

Severe cavitation load at the rotating disk facility is well manifested not only by figures 5 and 6, but also by the diagrams in figures 1-4. With sample surface area only 3.5 times higher than that at the vibrative rig, 10 times higher mass loss of the reference material (AISI 321) can be noticed after 360 minutes of exposure. A similar effect is shown by the time needed to reach the characteristic local peak of the reference material erosion rate to be ascribed to removing the major portion of the surface layer.

Tests at a rotating disk show a number of features. In addition to the fact that the cavitation load is very intense, there is also a large load gradient across the sample area. Cavitation load at the erosion zone edge is – according to our assessments - by two orders of magnitude lower than close to the specimen center. Therefore, only at the periphery, where the load is smaller, is the protective effect of the nitrided layer visible. This can be seen in figure 6, which shows SEM photographs of similar zones of titanium samples.

The traditional criterion for the erosion resistance of a material is the loss of its mass (volume) over a certain period of time. In the case of tests on a rotating disk, additional criteria for assessing the intensity of the impact of cavitation can be the dependence of the area of the erosion zone, as well as its depth, on the test time. From the analysis of the obtained geometric parameters of the cavitation erosion shape, a corresponding cavitation load distribution map can be created.

It should also be noted that in the case of a vibration test bench, where the cavitation load remains too high, much higher than in most industrial applications, a protective effect cannot be established.

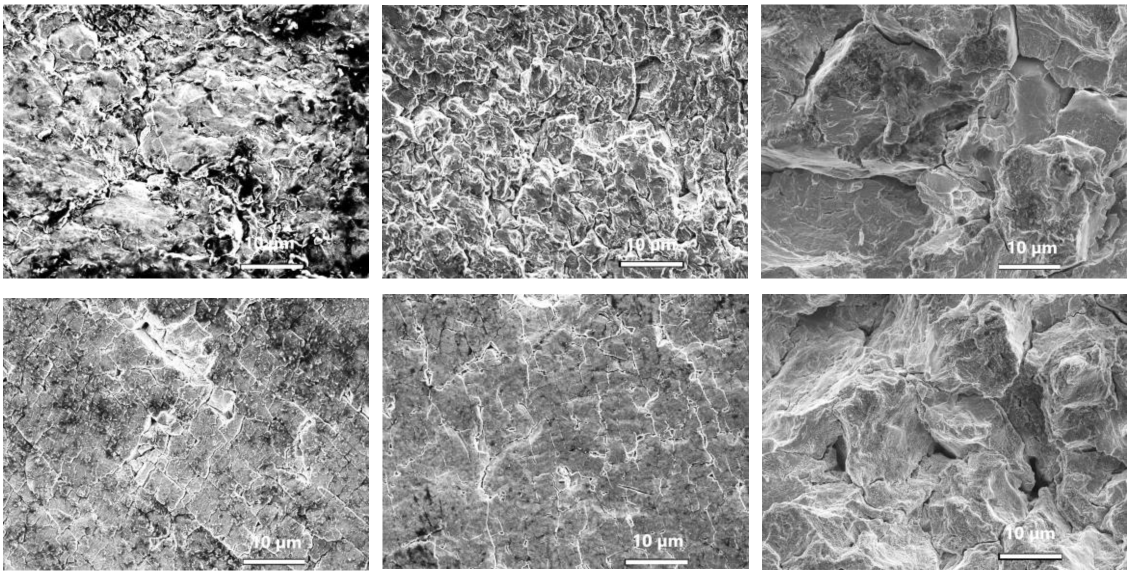

(a) (b) (c)

Figure 6. SEM images of samples titanium alloy after 360 min test duration. Top - without and bottom after nitriding. (a) -5 mm, (b) -8 mm and (c) -13 mm from the right edge to the center of the sample

A profound rise in erosion rate of the nitrided sample as tested at the vibrative rig can be noticed in the second hour of exposure. This seems to be the manifestation of removing the nitride surface layer. Given that the cavitation load on the vibration stand is high and uniform, the base material begins to deteriorate soon after the more brittle surface layer is quickly removed. The most probable reason is surface brittleness increased to the level prevailing over the increased hardness effect at high cavitation loads. A similar effect for the titanium alloy Ti6Al4V has been reported in reference [13]. The importance of choosing a suitable range of cavitation intensity for studying its effect on the stability of a passive film and understanding the mechanisms of repassivation of stainless steel, titanium, and nickel in an aggressive environment is shown in [14].

The above proves once more that cavitation erosion tests of structural materials and protective coatings or processed surface layers should be correlated in as much as possible with cavitation load. Contemporary instrumentation, such as digitized confocal microscopy, enables such research using even single samples with experimentally established erosive load. Development of relevant methodology is the purpose of studies conducted currently by the authors of this paper.

4. Conclusions

The kinetic dependences of erosion destruction of samples of stainless steel and titanium alloy VT3-1 in the initial state and after ion nitriding were obtained. A study of the microstructure, hardness and surface morphology was carried out. The relationship between mass loss and cavitation erosion time was measured and analyzed. The erosion rate of AISI 321 steel is seven times higher than that of titanium alloy. The effect of nitriding on the erosion rate of titanium alloys has been determined. Studies have shown that nitriding of titanium under selected processing parameters increases hardness, but does not lead to an increase in cavitation resistance, determined by mass loss. On the other hand, the eroded surface area of titanium after nitriding when tested on a rotating disk is smaller. Using optical and scanning electron microscopy, the protective effect of the modified layer under low cavitation loads is shown. The erosion rate on a rotating disk stand is significantly higher than during vibration tests. A large cavitation load gradient provides additional opportunities for analyzing the durability of materials and coatings using this method.

Acknowledgments

The study was supported by the program of international scientific cooperation between the Polish Academy of Sciences and the National Academy of Sciences of Ukraine (Project 46: "Advanced technologies of increasing cavitation and abrasion resistance of turbomachinery elements ", 2022-2024) as well as the European Fund for Displaced Scientists (grant EFDS-FL1-5) of the European Federation of Academies of Sciences and Humanities (ALLEA).

References

[1] Veiga C, Davim J P and Loureiro A J 2012 *Rev. Adv. Mater. Sci*. **32** 14
[2] Foldn T S and Aschmoneit F J 2023 *Physics of Fluids* **35** 081301
[3] Keil T, Pelz P F, Kadavelil J, Necker J, Moser W and Christ D 2011 Droplet impact vs. cavitation erosion *Proc. of WIMRC 3rd Int. Cavitation Forum* 4th-6th July (University of Warwick, UK) p 2011
[4] Hattori S and Takinami M 2010 *Wear* **269** 310
[5] Neville A and McDougall B 2001 *Wear* **250**(1–12) 726
[6] Hirotoshi S, Fuimo T and Hitoshi S 2020 *Wear* **462–463** 203518
[7] Kuzin I V and Kapustin S N 2020 *AIP Conf. Proc.* **2313** 060033
[8] Tsvetkov Y N, Fiaktistov Y O and Kudryavzeva Y R 2022 *J. Frict. Wear* **43** 20
[9] Jasionowski R, Polkowski W and Zasada D 2016 *Key Engineering Materials* **687** 117
[10] Steller J and Gireń B G 2018 International cavitation erosion test. Final report. *Zeszyty Naukowe IMP PAN* vol 560/1519/2015 ed F Jaroslaw (Gdansk: IMP PAN) p 104
[11] Safonov V, Zykova A, Steller J, Tolmachova G and Donkov N 2022 *J. Phys. Conf. Ser.* **2487** 012034
[12] Tuck J R, Korsunsky A M, Bhat D G and Bull S J 2001 *Surf. Coat. Technol.* **139** 63
[13] Kaspar J, Bretschneider J, Jacob S, Bonß S, Winderlich B and Brenner B 2007 *Surface Engineering* **23**(2) 99
[14] Hu J, Zhang L, Ma A, Mao P and Zheng Y 2022 *Metals* **12**(2) 198